Available online at www.sciencedirect.com

ScienceDirect

Procedia CIRP 14 (2014) 119 – 124

www.elsevier.com/locate/procedia

6th CIRP International Conference on High Performance Cutting, HPC2014

Prediction of Process Forces and Stability of End Mills with Complex Geometries

R. Grabowski[a]*, B. Denkena[a], J. Köhler[a]

[a]*Institute of Production Engineering and Machine Tools, Leibniz Universität Hannover, An der Universität 2, D-30823 Garbsen, Germany*

* Corresponding author. Tel.: +49-511-762-18331; fax +49-511-762-5115. *E-mail address:* Grabowski@ifw.uni-hannover.de

Abstract

In order to optimize the cutting performance of end mills, the geometry of such cutters is optimized by toolmakers constantly. As a result of geometric changes, process forces can be reduced, i.e. by serrated end mills. Tools with unequal helix angles can lead to an increase of process stability. In this paper, a method to calculate the process forces of end mills with complex geometries is presented. The method for calculating the process forces is designed for the application for stability analysis of end mill cutters with complex geometries. A basic introduction of the method for the stability prediction of such tools is given. Cutting forces of end mills are analyzed at incremental axial depth of cuts to show the influence of the tool geometry on the process forces. The comparison with experimental data verifies this method and shows the influence of further effects on the process forces. Furthermore, stability charts obtained with the Semi-Discretization Method are presented to show the potential of end mills with complex geometries regarding stability improvement.

Keywords:Milling; Process forces; Chatter; Stability charts; Serrated end mills; Unequal helix angles

1. Introduction

The dynamic behavior of the milling operation can lead to an unstable cutting condition, which often limits the actual potential of the machine tool in terms of productivity. One of the main reasons for instabilities are self-excited vibrations, referred to as chatter, which can arise during the machining process [1]. This dynamic behavior of the cutting process causes a modulation of the undeformed chip thickness, known as the regenerative effect, and can lead to a high amplitude of the process forces. As a result, the machined surface has a poor surface quality. Furthermore, the induced forces can damage the tool or even the spindle and machine.

By modifying the geometry of tools, the stability of milling operations can be increased. For example, tools with non-uniform tooth pitch or various helix angles influence the chip thickness and thus the occurrence of the regenerative effect [2]. Takuya et al. developed a computational method for a stability improving optimization of helix and pitch angles of end mills [3]. It must be noted that, depending on the process parameters, the modification of the tool geometry does not always increase the stability, as stated by Tlusty et al. [4]. They pointed out that tools with non-uniform pitch decrease the influence of the regenerative effect. The mode coupling mechanism, however, which is a forced vibration acting in two directions in the plane cut and can cause forced chatter vibrations, is not disturbed by this geometric modifications.

For roughing operations, end mills with serrated cutting edges are often used to increase stability. The characteristic of these tools is that the radius of the cutting edges have a periodic recession along the axial tool direction z (see Fig. 1).

In [5], Dombovari et al. presented a method to calculate process forces of serrated end mills. Furthermore, they applied the Semi-Discretization Method to obtain stability charts of serrated cutters. Koca and Budak chose a similar approach and proposed a method to design the optimal serration profile

doi:10.1016/j.procir.2014.03.101

leading to reduced forces and increased stability [6]. Merdol and Altintas solved the stability prediction in numerical domain [7].

In [8], the authors presented a method to calculate the process forces of tools with unequal helix angles. The following paper presents an extension of this method to compute the process forces of tools with serrated flutes. First, a brief mathematical description of this model will be given. Calculated process forces for an end mill with non-uniform helix angles and serrated cutting edge profiles, respectively, will be compared with experimental obtained forces. Resulting discrepancies between experimental and simulated forces are critically analyzed. Based on the mathematical model for process force calculation, numerical predicted stability charts for the used tools are presented.

Nomenclature

$h_{j,u}$	Undeformed chip thickness of the j-th tooth
$h_{\mathrm{stat},j,u}$	Stationary part of the undeformed chip thicknes of the j-th tooth
$h_{\mathrm{dyn},j,u}$	Dynamic part of the undeformed chip thicknes of the j-th tooth
$f_{j,u}$	Feed per tooth for the j-th tooth
f_{t}	Tooth passing frequency
f_{r}	Tool runout frequency
f_{δ}	Non-uniform helix angles frequency
φ_j, φ_u	Angular position of the j/u-th tooth
φ_{e}, φ_{a}	Entry and exit angle
r_j, r_u	Radius of the j/u-th tooth
$p_{j,u}$	Pitch angle between the j-th and u-th tooth
H_j	Set of all theoretically possible undeformed chip thickness of the j-th tooth
$g_{j,u}$	function to determine whether the j-th tooth is in cut or not
t	Time
n	Spindle speed
a_{e}	Width of cut
a_{p}	Depth of cut
δ_j	Helix angle of the j-th tooth
N_{t}	Number of teeth/flutes
$N_{\Delta z}$	Number of increments for the depth of cut
x, y, z	Coordinates of the fixed coordinate system
Δz	Incremental depth of cut
$\Delta\eta_j$	Displacement between the tool and the workpiece for the j-th tooth in the rotating coordinate system
$\theta_{j,u}$	Time delay of the j-th tooth
L	Wavelength of serration
a	recession of the flute for serrated end mills
$\mathbf{p}$	Vector with tooth pitch angles
$\mathbf{T}_j$	Rotation matrix for the j-th tooth
$\mathbf{q}$	Displacement vector consisting of the displacements in x and y direction of the workpiece and tool
$\mathbf{M}$, $\mathbf{D}$, $\mathbf{K}$	Mass, damping and stiffness matrix
K_{tc}, K_{rc}, K_{ac}	Cutting coefficient in the tangential, radial and axial direction
K_{te}, K_{re}, K_{ae}	Edge coefficient in the tangential, radial and axial direction

2. Derivation of the process forces

The following approach to derive the process forces of end mills is based on the mechanistic model by Altintas [8]. In order to extend this approach for end mills with non-uniform helix angles and varying recession of cutting edges, the undeformed chip thickness h needs to be redefined:

$$h_{j,u}(t,z) = h_{\mathrm{stat},j,u}(t,z) + h_{\mathrm{dyn},j,u}(t,z)\,. \tag{1}$$

$h_{\mathrm{dyn},j,u}(t,z)$ is the dynamical part of the undeformed chip thickness and accounts for the regenerative effect. $h_{\mathrm{stat},j,u}(t,z)$ is the static part and its value depends on the feed per tooth f_z and the angular position of the j th-flute. If the end mill has non-uniform helix angles or serrated flutes, the calculation of the undeformed chip thickness is more complex than for regular cutters. In the following sections the derivation of both parts of the undeformed chip thickness will be described.

2.1. Static part of the chip thickness

For end mills with serrated flutes or non-uniform helix angles the static part of the undeformed chip thickness can be calculated as:

$$h_{\mathrm{stat},j,u}(t,z) = f_{j,u}(z)\sin(\varphi_j(t,z)) + r_j(z) - r_u(z)\,. \tag{2}$$

$r_j(z)$ is the radius of the j-th flute along the z-axis (see Fig. 1). The radius of the flutes can lead to a decrease or increase of the chip thickness at certain angular positions $\varphi_j(t,z)$. Furthermore, a missed cut is possible. Thus, for the j -th flute u different chip thicknesses are calculated, with

$$\{u \in \aleph \mid 0 < u \le j\}. \tag{3}$$

In case of a missed cut, the next flute has to remove more material, and thus, the chip thickness increases due to an increase of the effective feed per tooth:

$$f_{j,u}(z) = f_z N_{\mathrm{t}} \frac{p_{j,u}(z)}{2\pi}\,. \tag{4}$$

N_{t} is the total amount of flutes. $p_{j,u}(z)$ is the pitch angle between the u th-flute and j th-flute. Fig. 1 shows the

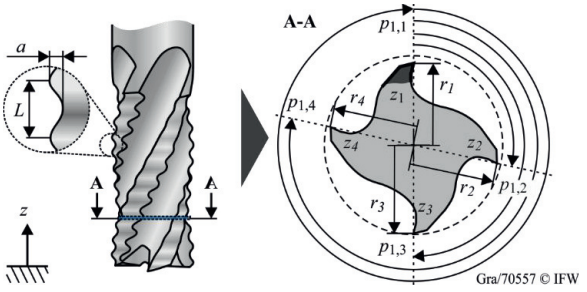

Fig. 1. Geometry of a serrated end mill cutter.

resulting non-uniform pitch for tooth $j = 1$ at a discrete position along the z-axis. The values of $p_{j,u}(z)$ can be calculated by:

$$p_{j,u}(z) = 2\pi + \varphi_u(t,z) - \varphi_j(t,z) - 2\pi\left\lfloor \frac{\varphi_u(t,z) - \varphi_j(t,z)}{2\pi} \right\rfloor. \quad (5)$$

To determine the actual chip thickness of tooth j, the minimum value

$$H_j(t,z) = \left\{ h_{\mathrm{stat},j,1}(t,z), \ldots, h_{\mathrm{stat},j,u}(t,z) \right\} \quad (6)$$

of all theoretical possible chip thicknesses has to be determined along the z-axis at every angular position. If the smallest value of $H_j(t,z)$ is smaller than 0, the flute is not in cut at the given position. This is represented by the following Heaviside-function:

$$g_{j,u}(t,z) = \begin{cases} 1, \min(H_j(t,z)) = h_{\mathrm{stat},j,u}(t,z) > 0 \\ \quad \wedge \varphi_e \le \varphi_j(t,z) \le \varphi_a \\ 0, \text{else} \end{cases}. \quad (7)$$

Furthermore, the angular position $\varphi_j(t,z)$ of the tooth must be between the entry angle φ_e and the exit angle φ_a.

2.2. Dynamic part of the chip thickness

The dynamic part of the chip thickness

$$h_{\mathrm{dyn},j,u}(t,z) = \Delta\eta_j(t - \theta_{j,u}(z)) - \Delta\eta_j(t) \quad (8)$$

represents the regenerative effect. $\Delta\eta_j(t)$ is the relative displacement between the tool and the workpiece in the rotating coordinate system of the tool and workpiece, respectively. This dynamic displacement is known as the outer modulation. $\Delta\eta_j(t - \theta_{j,u}(z))$ is the inner modulation and represent the wavy surface left behind by the previous tooth. Similar to eq. (4), the time delay $\theta_{j,u}(z)$ can be calculated as follows:

$$\theta_{j,u}(z) = n \frac{p_{j,u}(z)}{2\pi}. \quad (9)$$

n is the spindle speed. In accordance to the static chip thickness, eq. (7) is applied to determine which of the u dynamic cutting chip thicknesses for tooth j has to be considered.

3. Stability of end mills with complex geometries

In order to predict the stability of end mills with complex geometries, the Semi-Discretization Method is applied [10]. The mathematical description of the milling process is based on a time periodic delay differential equation (DDE). A derivation for this DDE for tools with non-unfirom pitch is given in [11]. This DDE is extended to account for non-uniform helix angles and changing radii of the flutes along the axial position:

$$\mathbf{M}\ddot{\mathbf{q}}(t) + \mathbf{D}\dot{\mathbf{q}}(t) + \left[\mathbf{K} + \sum_{j,u,=1}^{N_t} \sum_{i=1}^{N_{\Delta z}} \mathbf{Q}_{j,u}(t,z) \right] \mathbf{q}(t) = \sum_{j,u,=1}^{N_t} \sum_{i=1}^{N_{\Delta z}} \mathbf{Q}_{j,u}(t,z)\mathbf{q}(t - \theta_{j,u}(z)), \quad (10)$$

where $\mathbf{M}$, $\mathbf{D}$ and $\mathbf{K}$ are diagonal matrices, which contain the modal mass, damping and stiffness, respectively. The summation over the j teeth is necessary to take into account non-uniform pitch angles. With the index u the dynamic undeformed chip thickness for end mills with unequal helix angles or recessed flutes, based on eq. (7) and (8), can be described

$$\mathbf{Q}_{j,u}(t,z) = \mathbf{T}_j(t,z) \begin{bmatrix} 0 & K_{tc} \\ 0 & K_{rc} \end{bmatrix} \mathbf{T}_j^{-1}(t,z) \Delta z g_{j,u}(t,z), \quad (10)$$

whereas $\mathbf{T}_j(t,z)$ is a rotation matrix to transform coordinates between the fixed and the rotating coordinate system of the tool and workpiece, respectively. The axial depth of cut is approximated by a summation with $\Delta z = a_p / N_{\Delta z}$. In the next steps, this system is discretized and the corresponding system vector and matrix are expanded. The stability of the system can be determined by the eigenvalues of the expanded system [11, 12].

4. Experimental setup

Two different end mills, with a diameter D = 16 mm and 4 teeth, are used for the comparison between the experimental and calculated process forces. Tool 1 has non-uniform helix angles. The diametrical opposed flutes have the same helix angle $\delta_1 = \delta_3 = 35°$ and $\delta_2 = \delta_4 = 38°$, respectively. Tool 2 has a serrated profile, a non-uniform pitch $\mathbf{p}$ = [93° 87° 93° 87°] and a uniform helix angle of $\delta = 45°$. The wavelength L of the serration is 2.1 mm with a maximum recession a of the flute of 0.3 mm.

Fig. 2 shows an illustration of the experimental configuration. An AL7075-T651 work material is mounted on a Kistler 9257B force plate. The work piece has an overhang, which allows to shift the height at which the flutes are in cut. For tool 1 two different cutting heights are analyzed. At Position 1, the tool is shifted 2 mm to prevent an influence of the corner radius R at the tool tip on the measured process forces. Position 2 starts at a height of 24 mm. This permits on

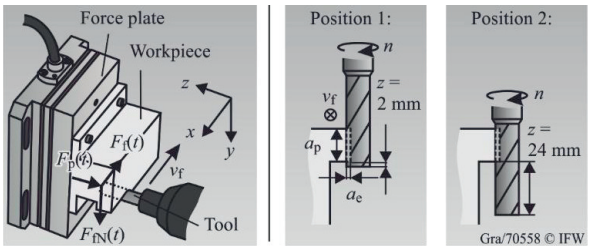

Fig. 2. Experimental configuration for force measurement at two different axial positions

the one hand to observe how the process forces change along the axial position due to the non-uniform helix angles. On the other hand, due to the shortened effective tool length, the influence of dynamic effects of the machining process should be minimized.

Experiments are conducted on a 4 axis horizontal milling machine center. The up milling operation is carried out with a radial and axial immersion of $a_e = 1$ mm and $a_p = 8$ mm, respectively, at a spindle speed n of 300 min^{-1}. For the feed per tooth f_z a value of 0.1 mm was chosen. Furthermore, full slot milling operations are conducted to obtain the cutting and edge force coefficients (see Table 1).

Table 1. Cutting force coefficients.

Coefficients	Unit	Tool 1	Tool 2
[K_{tc} K_{rc} K_{ac}]	[N/mm²]	[541 10 298]	[821 365 396]
[K_{te} K_{re} K_{ae}]	[N/mm]	[16 11 1.4]	[20 13 1.4]

5. Comparison between experimental and predicted process forces

In general, dynamic effects in the form of vibrations superimpose the measured cutting forces. The tooth entry is like a sudden impulse, and thus, the natural frequency of the work piece or the force plate can be excited. Furthermore, looking at the resulting forces for one revolution, there might be slight differences of the process forces between the previous and the next revolution. In order to minimize the mentioned effects, the measured forces are divided into the length of one revolution. Next, the forces for the various single revolution are superimposed and the mean value for one revolution is calculated. The result of this method is shown for tool 1 at Position 1 in Fig. 3. For the original signal, one tool revolution at a random time position was chosen. As shown, the filter method minimizes the influence of vibrations. For the force in feed normal direction F_{fN} there is a greater visible difference between the filtered and the original signal at the beginning. With the proposed method, force random variations are filtered.

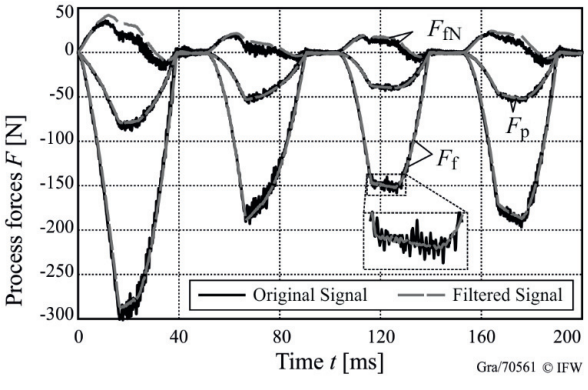

Fig. 3.Original and filtered signal of the experimental obtained process forces (tool 1, Position 1 ($z = 2$ mm).

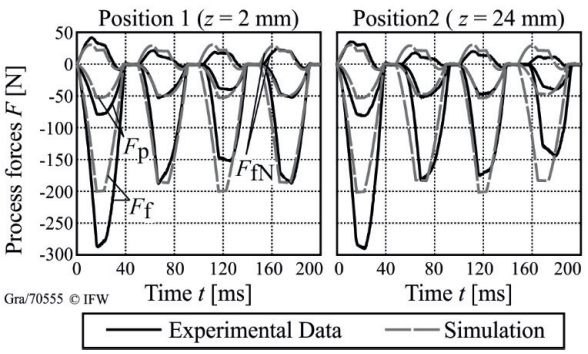

Fig. 4. Experimental and simulated cutting forces for the end mill with unequal helix angles (tool 1).

As the signal shows, the difference in the force amplitude between the singular teeth exceeds for the force in feed direction F_f a value of over 100 N. Although non-uniform helix angle cause altering amplitudes, this difference is too high. Furthermore, the diametrical arranged teeth of tool 1 have the same helix angle. Thus, every second tooth should have the same force amplitude. Fig. 4 shows the process forces of tool 1 for Position 1 and Position 2. The simulated process forces show the expected altering of the force amplitudes. At Position 2, this difference increases slightly. Looking at the experimental data, the values between Position 1 and Position 2 differs, too. In order to find out the causes for this amplitude differences, the measured and simulated forces in feed direction are analyzed in the frequency domain, shown in Fig. 5. The highest peak at 20 Hz is the tooth passing frequency f_t . For the measured signals, a peak at 5 Hz is visible. This frequency f_r corresponds to one revolution of the tool (n = 300 min^{-1}) is caused by the tool runout. The height of this peaks provides information about the influence of the tool runout on the measured process forces. A measurement of the actual radius of the teeth showed differences between the singular teeth, and thus, it can be assumed that the highest part of the force amplitude discrepancies is caused by tool runout. The influence of tool runout on process forces was analyzed by Krüger and Denkena in [13]. Their results verifies this assumption. Due to

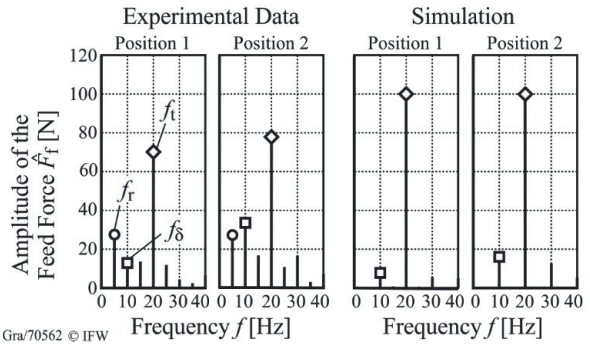

Fig. 5. Signal of the experimental and calculated cutting forces in the frequency domain

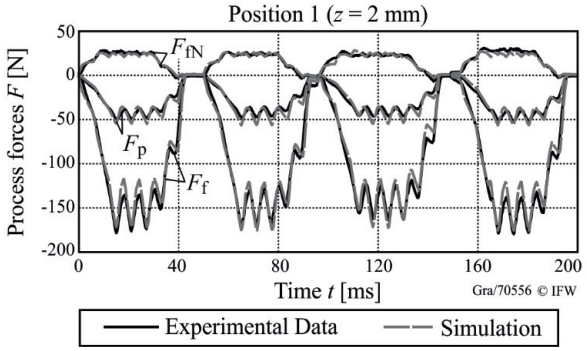

Fig. 6. Experimental and simulated cutting forces for the end mill with serrated cutting edges (tool 3).

the fact that tool runout is not taken into account in the simulation, no peak occurs at 5 Hz in the frequency domain of the calculated forces. Looking at the frequency signal of the measured and calculated forces at Position 1, a further peak occurs at f_δ = 10 Hz. This peak corresponds to a half revolution of the tool. Due to the fact that the diametrical positioned teeth have the same helix angle, it can be assumed that this frequency shows the influence of the helix angle on the process forces. Furthermore, compared to Position 1, the amplitude of the frequency f_δ at Position 2 increases for the measured and calculated forces, respectively. At higher tool position, the difference of the pitch between the teeth increases, and thus, this explains the increase of amplitude.

The resulting process forces of the serrated end mill (tool 2) are shown in Fig. 6. Due to the high value for the depth of cut a_p and low value for the width of cut a_e, the shape of the serration is reflected in the force signal. The force amplitude is almost the same for all teeth, and thus, tool runout analysis can be neglected. Furthermore, the calculated process forces show a good agreement with the experimental data. Compared to tool 1, the serrated end mill leads to lower averaged process forces. As mentioned by Dombovari et al., serrated flutes cut thicker chips which leads to a decrease of the averaged process forces [5].

6. Stability charts for end mills with complex geometries

For the prediction of the stability charts, the frequency response functions of the tool in x and y direction are estimated by a tip test. It is assumed that the work piece is rigid. For both directions, the two modal parameters with the highest amplitude are considered for the stability prediction (see Table 2). Fig. 6 shows the resulting stability charts. To show the effect of non-uniform helix angles on the stability limit, a stability chart for tool 1 is calculated and the helix angle is set to a constant value of δ = 35° for all teeth (tool 1').

As expected, the stability of the tool 1' has the lowest values at almost all spindle speeds compared to tool 1 and 2. Due to the changing time delays in axial direction of the end mill with unequal helix angles, the regenerative effect is attenuated and thus, the stability increases. The attenuation of

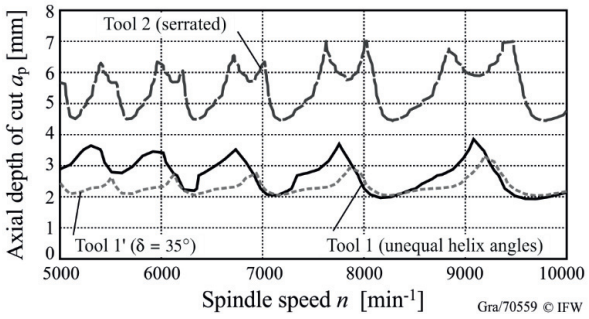

Fig. 7. Stability charts for the three different end mills.

the regenerative effect is even higher for the serrated end mill, which leads to a high stability limit for the investigated spindle speed range. The results show the importance of the tool geometry on the stability. For tool 2, the tool runout effect was not taken into account. Further analysis are necessary to show a possible influence of the tool runout on the stability. This requires the measurement of the actual radii of the teeth along the tool axis. Furthermore, experimental stability test must be carried out to verify the stability charts with experimental values

Table 2. Modal parameters of the tool in x - and y -direction.

Direction	Mode No.	m [kg]	d [Ns/m]	k [N/µm]	f_0 [Hz]
x	1	0.16	194	45	2669
x	1	0.08	67	45	3774
y	2	0.11	216	55	2513
y	2	0.17	60	42.4	3558

7. Conclusion

End mills with complex geometries, e.g. non-uniform helix angles or serrated flutes, can improve the stability, and thus, the productivity of milling operations. The mechanics and dynamics of cutters with complex geometries are investigated in this paper. The comparison between the experimental obtained and calculated process forces showed that for tools with unequal helix angles further effects, i.e. tool runout, can lead to discrepancies in the prediction. For serrated end mills the experimental obtained and calculated process forces are in good accordance. By applying the Semi-Discretization Method, stability charts for the investigated tools were predicted. The results show that the geometry have a great influence on the process stability. To validate the predicted stability charts, experimental stability tests are necessary. Additionally, further investigations should take tool runout effects into account for the prediction of stability charts.

Acknowledgements

This work has been supported by the Ministry for Science and Culture of Lower Saxony (MWK) within the excellence cluster “Pro³gression”.

References

[1] Tobias SA, Fishwick W. Eine Theorie des regenerativen Ratterns an Werkzeugmaschinen. In: Maschinenmarkt 17. 1956. p. 15-30.
[2] Sims N, Mann B, Huyanan S. Analytical prediction of chatter stability for variable pitch and variable helix milling tools. In: Journal of Sound and Vibration 317 (3-5). 2008. p. 664-686.
[3] Takuya K, Suzuki N, Hino R, Shamoto E. A novel design method of variable helix cutters to attain robust regeneration suppression. In: Procedia CIRP 8. 2013. p. 362-366.
[4] Tlusty J, Zaton W, Ismail F. Stability Lobes in Milling. In: CIRP Annals – Manufacturing Technology 32 (1). 1983. p. 309-313.
[5] Dombovari Z, Altintas Y, Stepan G. The effect of serration on mechanics and stability of milling cutters. In: International Journal of Machine Tools & Manufacture 50. 2010. p. 511-520.
[6] Koca R, Budak E. Optimization of Serrated End Mills for Reduced Cutting Energy and Higher Stability. In: Procedia CIRP 8. 2013. p. 569-574.
[7] Merdol D, Altintas Y. Mechanics and Dynamics of Serrated End Mills, In: Transactions of the ASME, Journal of Manufacturing Science and Engineering 126(2). 2004. p. 317-326.
[8] Grabowski R, Köhler J, Denkena B. Process force and stability prediction of end mills with unequal helix angles. In: Lecture Notes in Production Engineering. 2014. p. 91-96.
[9] Altintas Y. Manufacturing Automation - Metal Cutting Mechanics, Machine Tool Vibrations, and CNC Design. 1st ed. New York: Cambridge University Press; 2000.
[10] Insperger T, Stepan G. Semi-discretization of delayed dynamical systems. In: ASME 2001 Design Engineering Technical Conferences and Computers and Information in Engineering Conference. 2001. p. 1-6.
[11] Sellmeier V, Denkena B. Stable islands in the stability chart of milling processes due to unequal tooth pitch. In: International Journal of Machine Tools & Manufacture 51. 2011. p. 152-164.
[12] Kleckner J. Ein Beitrag zur Analyse dynamischer Interaktionen bei selbsterreungsfähigen Drehbearbeitungsprozessen. PhD Thesis. Technische Universität Darmstadt. 2001.
[13] Krüger M, Denkena B. Model-based identification of tool runout in end milling and estimation of surface roughness from measured cutting forces. In: International Journal of Advanced Manufacturing Technology 65 (5-8). 2013. p. 1067-1080.